A case study concerning vertical motions and precipitation at a frontal zone

By LARS OREDSSON, *Institute of Meteorology, University of Stockholm*[1]

(Manuscript received September 22, 1964)

ABSTRACT

On a synoptic scale the distributions of vertical velocities and precipitation in connection with a certain frontal zone have been investigated utilizing data from one of the meteorological world intervals of the I.G.Y.

Vertical velocities of about 10–30 cm sec^{-1} in the middle troposphere, *upward* in the *cold air* and *downward* in the *warm air*, have been computed and the results are in very good agreement with the distributions of the observed humidity and the observed and computed precipitation.

Introduction

Three-dimensional synoptical-aerological analysis has to a great extent suffered from the lack of sufficiently dense networks of observations both in space and time. 12 hours, which is the normal time interval, is for most problems altogether too long to enable a three-dimensional analysis of the variation of the meteorological elements with time to be made. Examples can be given of earlier completed investigations of the vertical velocities on the synoptical scale, which were calculated as average values during 12-hour-intervals. Under such lengths of time there is a considerable risk that upward and downward movements wholly or partly manage to compensate each other, with the result that the real features of the vertical circulation on this scale can be concealed.

During the International Geophysical Year's meteorological world interval the wishes for denser networks of observations were fulfilled by quarterly 10-day periods. During those days not only had the network increased in size by the addition of new stations, but also a great number of ordinary aerological stations made measurements every 6 hours.

Data from the second meteorological world interval of the I.G.Y., i.e. 18–27th September 1957, forms the basis for this investigation, and, at least in the more important areas, the observations have been controlled with meticulous care.

1. The weather situation and the purpose of the investigation

The weather situation, which is illustrated in Figs. 1–5, will be described in greater detail in a later paper on baroclinic zones in the westerlies. The frontal zone, which concerns this investigation is to be found in the middle and upper troposphere over Scandinavia with a fairly slow movement south-eastwards. From the cross-sections in Fig. 3 and the temperature diagrams in Fig. 12, it can be seen that the frontal zone is well developed in the middle troposphere whilst it can be hardly said to exist as a limited zone in the extreme lowest layers. The front is not indicated on the weather-maps in Figs. 1 and 4, but is very apparent at the 500 mb level in Figs. 2 and 5. In the middle trophosphere the front has a width of more than 200 km and an isobaric temperature gradient of about 6°C/100 km. Between Gardermoen and Gothenburg (Göteborg) the front moves very slowly southwards with a speed of 15–20 km/hour, but after passing Gothenburg it increases its speed over southern Sweden. The frontal zone is very steep and has a slope of about 1:40 through the whole troposphere. Over Stockholm the front lies almost still and it takes about one day and night for the system to pass from west to east in the middle troposphere; this can be seen from the temperature diagrams in Fig. 12. The characteristics of the frontal zone and its windsystem can be

[1] Contribution No. 170 from the Institute of Meteorology, University of Stockholm.

studied in greater detail in the different representations which are illustrated and they need for our purpose no further comments.

On the weather-maps for 23rd and 24th September, 1200 GMT, Figs. 1 and 4, the polar front can be seen with its waves and areas of precipitation, which can be said to have developed and moved to a large extent according to the rules once set out by the Bergen school. It is probable that a forecast concerning weather and precipitation made by an experienced meteorologist for the area influenced by the polar front would have been rather successful. The areas of precipitation over Europe during the period 0600 to 1800 GMT on 24th September can be seen in Fig. 6. There occurs over Scandinavia another type of precipitation region which is not connected at all to any front at ground level. This region of precipitation has been displaced south-eastwards during the last 24 hours. Hardly any standard atmospheric models can describe this type of precipitation.

From a study of the 500 mb analysis on 24th September, 1200 GMT, Fig. 5, it is apparent that the region of precipitation in question lies in the immediate vicinity of the frontal zone described above. Based solely on this analysis, however, the precipitation may not be regarded as a result of warm air rising at the frontal surface. With further study of the situation in the precipitation region in relation to the observed distribution of the humidity in the cold and warm air at the front, it is obvious that in all likelihood all the precipitation is generated in the cold air.

Precipitation during the period 0600 to 1800 GMT on 24th September over Sweden has been analysed with the help of the denser network of climatological stations, which give 24-hour records of the precipitation. As further help in the analysis, weather-maps for every third hour were utilized, together with a less number of stations which made weather observations every hour. Substantial amounts of rain had been reported, and according to the observations the rain was not of the showery or intermittent types. The result of the analysis is illustrated in Fig. 6.

The purpose of the investigation is to attempt to calculate the distribution of vertical velocities at the frontal zone, and from this the horizontal divergence. From the distribution of divergence the precipitation can be computed using certain assumptions, and we thus obtain a check on the results in the area in which upward motions occur. In the region of downward movements it is difficult to carry out a similar verification, but the humidity records can to a certain extent be used.

The calculations have only been carried out at the points A, B, C and D which are indicated in Fig. 6. A and B represent the central and outer parts respectively of the precipitation region in the cold air. C lay in the warm air and had no rain from 0600 to 1800 GMT on 24th September. In the same period D lay for the first 6 hours in the warm air, but in the last 6 hours the warm air had been replaced by cold air; there was no precipitation at D. The reason for the choice of period has been the confidence in the analyses of the centre of the low, the topography of the different pressure surfaces and the positions of the frontal zone.

2. The principles used for the computation of the vertical velocities

The choice of computing method depends to a great extent on the type of observational material available, but it is also dependent upon the kind of processes which occupy the region in question.

When there is insufficient wind data over the area in question the vertical velocity, $\omega = dp/dt$ in the p-system, cannot be calculated directly from the equation of continuity, $\partial\omega/\partial p = -(\mathrm{Div}_H \mathbf{v})_p$ which otherwise would be the simplest method.

The computation of the vertical velocity based on the condition of dry-adiabatic processes must be regarded as very uncertain within the areas of upward air motions in connection with precipitation. Of course, one of the so-called adiabatic methods can be used with advantage for downward air motions and also perhaps with upwards motions in the higher layers having low temperatures, if the form of observed data in other respects is suitable for the method in question.

More generally, attention should be paid to the importance of making a careful study of the utilized basic equations, the range of their validity and their sources of error so that the accuracy of the results is not lost through wrong usage. It is possible that in computing

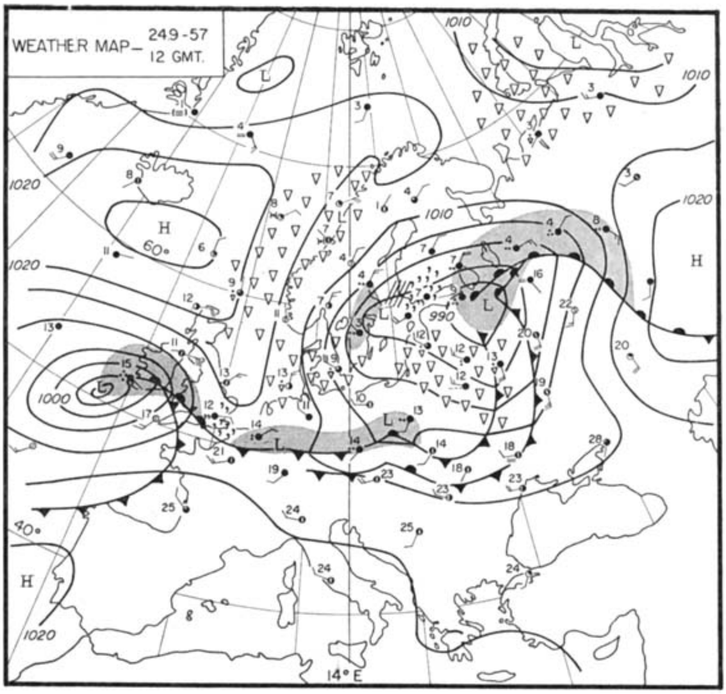
WEATHER MAP – 24.9-57
12 GMT.
14° E

FIG. 4

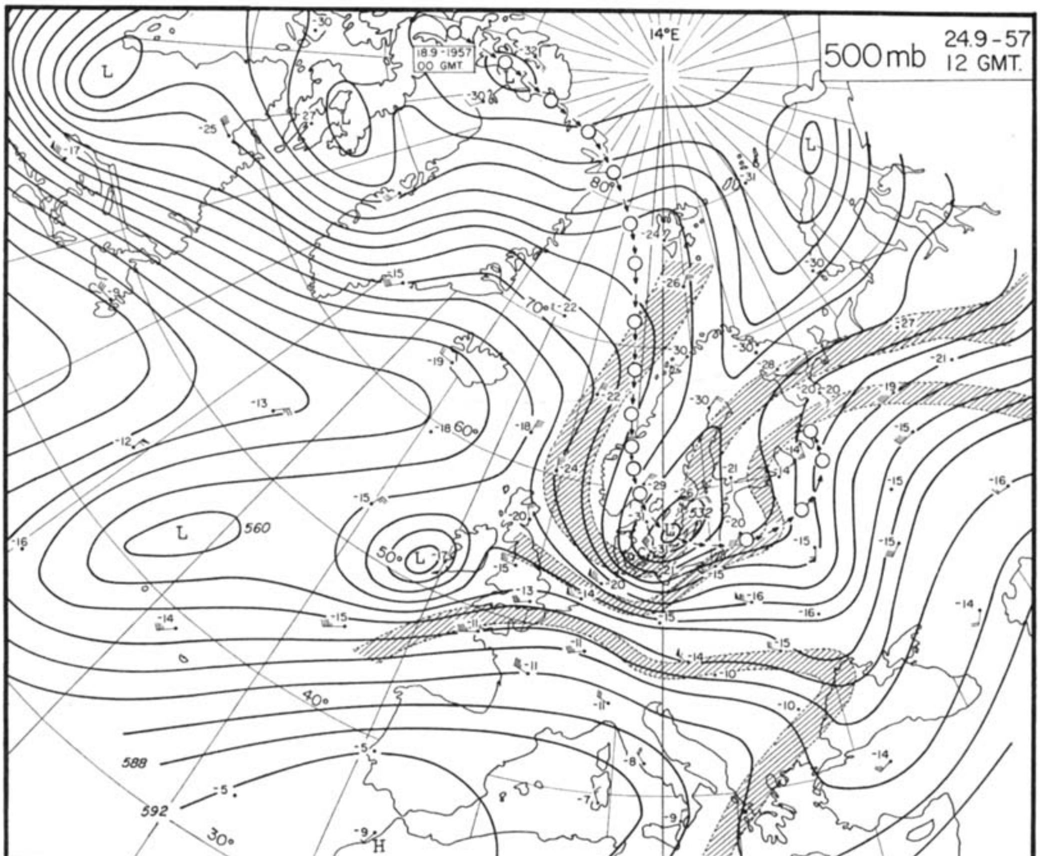
500 mb 24.9-57
12 GMT.
18.9-1957
00 GMT
14°E

FIG. 5

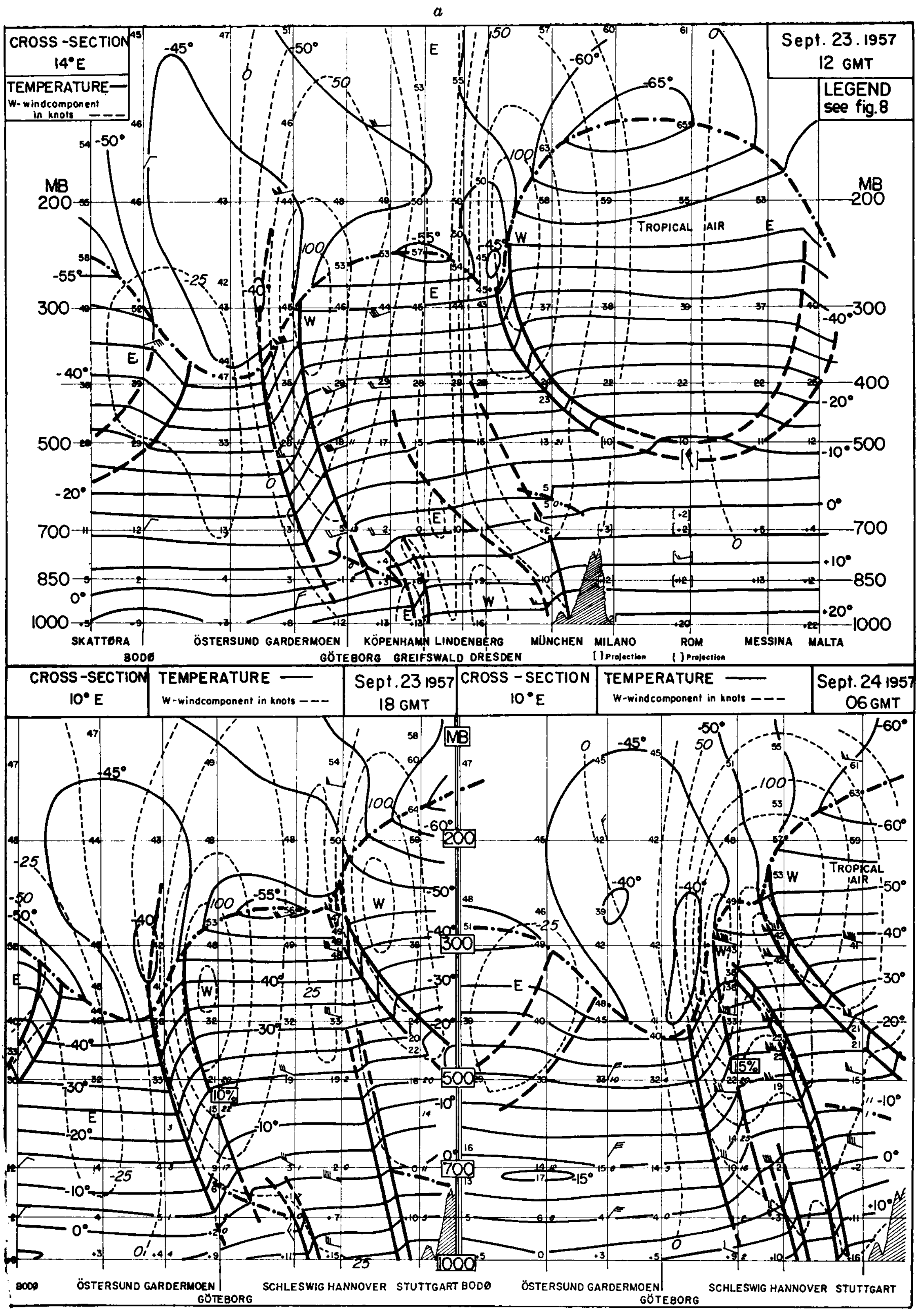
a
CROSS-SECTION 14°E
TEMPERATURE
W-windcomponent in knots
Sept. 23. 1957 12 GMT
LEGEND see fig.8
MB
TROPICAL AIR
SKATTØRA
BODØ
ÖSTERSUND GARDERMOEN
GÖTEBORG
KÖPENHAMN LINDENBERG
GREIFSWALD DRESDEN
MÜNCHEN MILANO
ROM
MESSINA MALTA
[ ] Projection
( ) Projection
CROSS-SECTION 10° E
TEMPERATURE
W-windcomponent in knots
Sept. 23 1957 18 GMT
CROSS-SECTION 10° E
TEMPERATURE
W-windcomponent in knots
Sept. 24 1957 06 GMT
TROPICAL AIR
BODØ
ÖSTERSUND GARDERMOEN
GÖTEBORG
SCHLESWIG HANNOVER STUTTGART
BODØ
ÖSTERSUND GARDERMOEN
GÖTEBORG
SCHLESWIG HANNOVER STUTTGART
b
c

FIG. 3

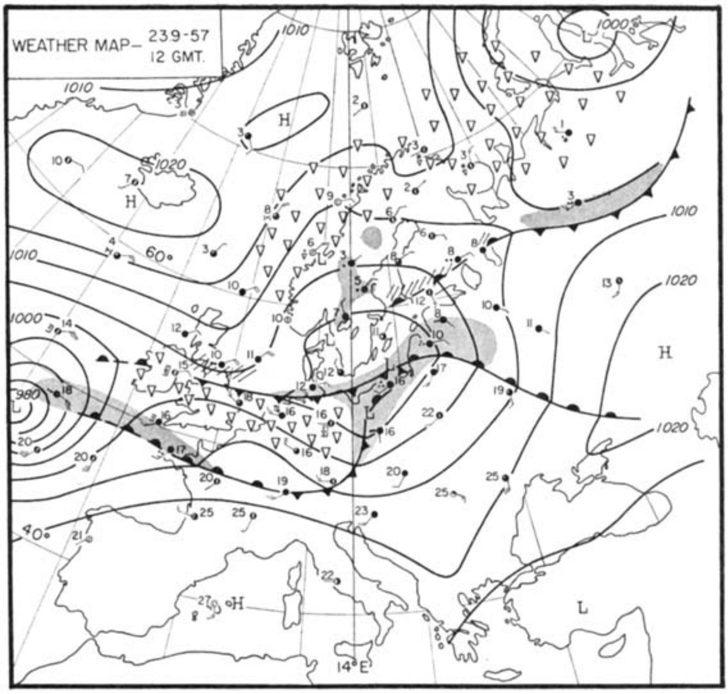

FIG. 1

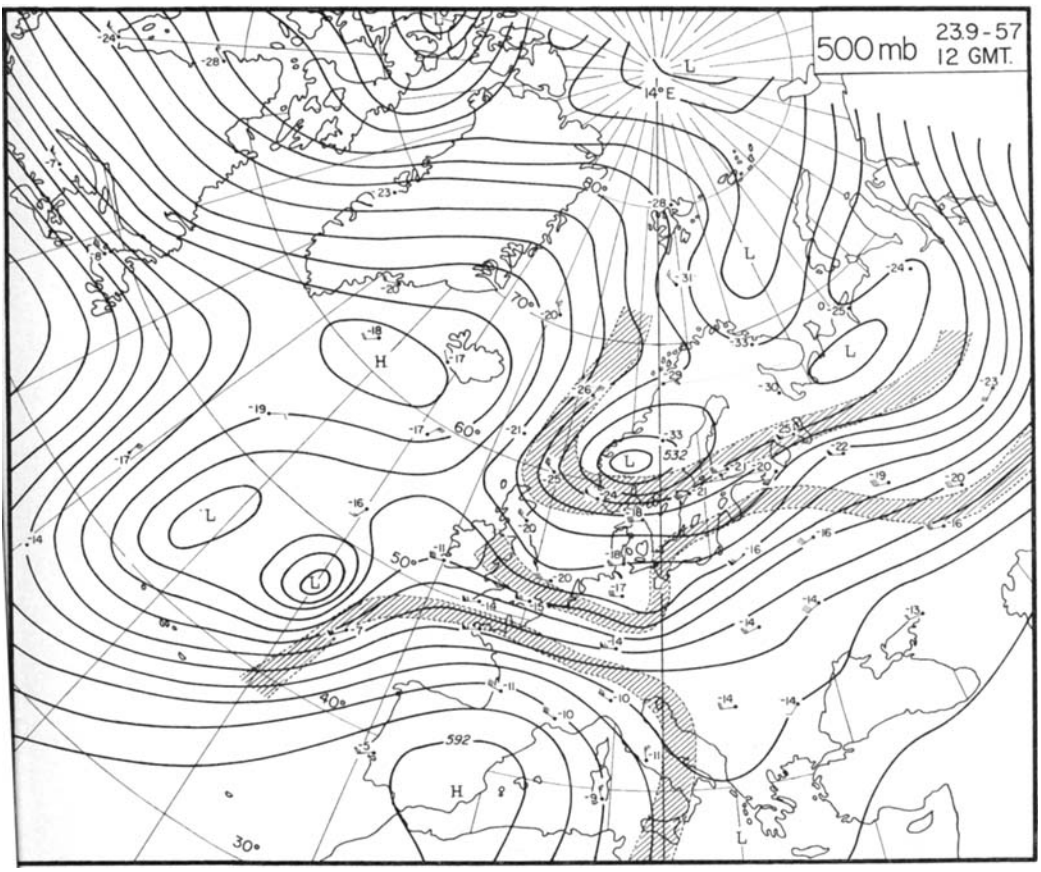

FIG. 2

vertical velocities it is preferable to use different methods for different places and different times. This is certainly also the case under the presumption that the choice of method is made so carefully as possible and in such a way that the applicable approximations in every special case are brought to a minimum.

For the present investigation only dynamical principles have been applied, and the formula used for the computations of the vertical velocities is derived from the hydrodynamic equations of motion and the equation of continuity. Hereby, for example, all the assumptions concerning the thermodynamics of the atmospheric processes have been avoided.

The complete vorticity equation, neglecting frictional effects, can be written as follows using the pressure (p) as the vertical coordinate:

$$\frac{d\eta}{dt} = \eta\frac{\partial\omega}{\partial p} + \mathbf{k}\cdot\frac{\partial \mathbf{v}_H}{\partial p}\times(\nabla_H\omega)_p; \tag{1}$$

$\eta = \zeta + f$ is the vertical component of the absolute vorticity, ζ is the vertical component of the relative vorticity and f is the Coriolis parameter. Regarding the last term in (1), the "tilting term", at every pressure surface this becomes zero in the areas of maximum vertical velocity and it is probable that the points A and B lie very near the area of maximum upward motion. Moreover, the isobaric temperature gradient over these regions (see Fig. 8a) is probably small and thereby, in the case of approximate geostrophic balance, the term $\partial \mathbf{v}_H/\partial p \approx \partial \mathbf{v}_g/\partial p$ is brought to a minimum. This last condition even applies to the point C. At these points this term therefore may be neglected. The situation at the point D is more doubtful and calculations at this point for the higher levels gave rather unreasonable results. However, the point D lies wholly in warm air at 0600 GMT and wholly in cold air at 1800 GMT (see Figs. 7 and 9). The used values for 1200 GMT did not justify a complete neglection of the "tilting term".

For our purpose the vorticity equation can now be written in the simplified form:

$$\frac{d\eta}{dt} = \left(\frac{\partial\eta}{\partial t}\right)_p + \mathbf{v}_H\cdot(\nabla_H\eta)_p + \omega\frac{\partial\eta}{\partial p} = \eta\frac{\partial\omega}{\partial p}$$

or

$$\frac{\partial}{\partial p}\left(\frac{\omega}{\eta}\right) = \frac{1}{\eta^2}\left[\left(\frac{\partial\eta}{\partial t}\right)_p + \mathbf{v}_H\cdot(\nabla_H\eta)_p\right]. \tag{2}$$

The equation (2) is now integrated stepwise along the vertical, and if the integration interval is not taken too large the assumption of evaluating the right-hand side as a linear function of pressure may be justified.

Integration of (2) between the pressure levels 1 and 2 gives:

$$\omega_2 \approx \frac{\eta_2}{\eta_1}\omega_1 - \eta_2(p_1-p_2)\tfrac{1}{2}\left\{\frac{1}{\eta_2^2}\left[\left(\frac{\partial\eta_2}{\partial t}\right)_{p_2} + \mathbf{v}_{H_2}\cdot(\nabla_H\eta_2)_{p_2}\right] + \frac{1}{\eta_1^2}\left[\left(\frac{\partial\eta_1}{\partial t}\right)_{p_1} + \mathbf{v}_{H_1}\cdot(\nabla_H\eta_1)_{p_1}\right]\right\}. \tag{3}$$

This is the formula which is used for the computations. The vertical velocity at one level is determined through the knowledge of the vertical velocity in another level together with the values of wind and vorticity, and the local changes in the vorticity with time at both levels.

3. The determination of the necessary parameters from data material and a discussion of the approximations

A. The vertical velocity at the lower boundary of the aircolumn

The relationship between the vertical velocity in the z-system, w, and ω is expressed through the equation $gw = (\partial\Phi/\partial t)_p + \mathbf{v}_H\cdot(\nabla_H\Phi)_p - \alpha\omega$ where Φ is the geopotential of the pressure surface and α is the specific volume. Since the error in the final calculations of the vertical velocity would clearly appear to exceed 1 cm sec^{-1} those terms in this formula, which only in exceptional cases reach such values, can be neglected.

If so great a value of the pressure surface's change of height as 300 gpm in 6 hours, corresponding to 15–20 mb in 3 hours at ground level, is assumed, then the expression $1/g\,(\partial\Phi/\partial t)_p \approx 1.4$ cm sec^{-1}. The second term on the right-hand side becomes zero in the case of geostrophic balance. Assuming an angle of 60° between the vectors

$$|\mathbf{v}_H| = 50 \text{ m sec}^{-1}$$

and $$|(\nabla_H\Phi)_p| = 40 \text{ gpm per 100 km}$$

the expression $(1/g)\ \mathbf{v}_H \cdot (\nabla_H \Phi)_p$ gives a value of about 1 cm sec^{-1}. (These values may be found in the regions of entrance or exit in connection with a jetstream at higher levels. At ground level the angle can naturally be less, but then the wind velocity is also less.)

Both these terms in the above expression can, without losing too much accuracy, be neglected when the order of magnitude of the calculated vertical velocity becomes 10 cm sec^{-1} (see Figs. 10–11). Thus the following relationship is obtained:

$$\omega \approx -\frac{\alpha}{g}\omega \tag{4}$$

which has been used later in the re-calculation of ω to w. If the effect of the earth's topography on the vertical velocity in the areas around the chosen points where the surface pressure is about 1000 mb, is wholly neglected, then $w_0 \approx \omega_{1000\ \text{mb}} \approx 0$.

B. THE SUBSTITUTION OF THE WIND AND VORTICITY BY THE GEOSTROPHIC WIND AND GEOSTROPHIC VORTICITY

Altogether, the terms in (3) include the vorticity or its derivatives. When the direct wind observations are lacking in the material over the area in question the vorticity has been replaced by the geostrophic vorticity. Thus,

$$\eta \approx \eta_g = \zeta_g + f = \mathbf{k} \cdot (\nabla_H \times \mathbf{v}_g)_p + f \approx \frac{1}{f}(\nabla_H^2 \Phi)_p + f,$$

at which the variation in f with latitude is neglected—a quite unimportant approximation in this case. Through the passage from differentials to finite differences the geostrophic vorticity is computed in a grid from the height fields of the successive pressure surfaces. The distance between the points in the used grid is discussed later.

The absolute topographies for the 1000, 850, 700, 500 and 300 mb surfaces (in certain cases even 200 and 100 mb) have been analysed with extreme care for every 6 hours and in so doing, the relative topography, amongst other things, was utilized. Several vertical cross-sections were constructed and the structure of the broad frontal zone was studied. The greatest possible continuity in time and space was sought after. The errors in the height values increase of course with height as do the observational errors, which is the reason why the 200 and 100 mb levels with a desired reasonable accuracy in the results cannot normally be used for the following vorticity determination.

The field of the absolute geostrophic vorticity calculated at all grid points was later analysed. For this, several vertical cross-sections in the actual region were constructed and analyses made of them in order to obtain a good continuity of the three-dimensional vorticity distribution. This careful and time-consuming three-dimensional analysis seems to be necessary, otherwise a chaotic final picture would easily ensue of the vertical distribution of the vertical velocity and the isobaric divergence.

Before we proceed, the arising error in the ω-computation depending on the geostrophic approximation should be considered in somewhat more detail. On the basis of the equation (3) for the calculation of the vertical velocity it can be immediately stated that in the areas of great anticyclonic relative vorticity, for instance with a value of η_g between 0 and $0.8 \cdot 10^{-4}$ sec^{-1}, the method gives exceedingly uncertain results, independently of whether a geostrophic balance prevails or not. On the other hand too great a value of η_g is often found in the frontal zones, the areas of which for previously stated reasons (the neglection of the "tiltingterm") are best avoided.

The following discussion deals with the atmosphere above the frictional layer. It is assumed that $|\mathbf{v}_H| = k|\mathbf{v}_g|$, where in general, $0.5 < k < 1.5$, i.e. the geostrophic assumption implies an over or under-estimation of the magnitude of the true wind. Inside the area under calculation a unitary deviation in the direction of the true wind from that of the geostrophic wind does not influence the relative vorticity since this is independent of the orientation of the co-ordinate system. All terms in the basic formula (3) contain the value of the absolute vorticity at two levels. Now, if the integration interval is chosen not to be too large it can be accepted that to a great extent the over or under-estimation of the true wind is the same at both levels (this would seem to be a good approximation if the frontal zones themselves are avoided), i.e.

$$|\mathbf{v}_{H_2}| = k_2|\mathbf{v}_{g_2}|, \quad |\mathbf{v}_{H_1}| = k_1|\mathbf{v}_{g_1}| \quad \text{and} \quad k_2 \approx k_1 = k.$$

TABLE 1. *A comparison between certain expressions described in the text above.*

Term	True values	Geostrophical values
I	$\frac{k\zeta_{g_2}+f}{k\zeta_{g_1}+f}$	$\frac{\zeta_{g_2}+f}{\zeta_{g_1}+f}$
II	$\frac{k}{k\zeta_{g_2}+f}\cdot A_2$	$\frac{1}{\zeta_{g_2}+f}\cdot A_2$
III	$\frac{k\zeta_{g_2}+f}{k\zeta_{g_1}+f}\cdot\frac{k}{k\zeta_{g_1}+f}\cdot A_1$	$\frac{\zeta_{g_2}+f}{\zeta_{g_1}+f}\cdot\frac{1}{\zeta_{g_1}+f}\cdot A_1$

The terms which are influenced by the absolute vorticity can for the purpose in question be written in the following form:

$$\mathrm{I}=\frac{\eta_2}{\eta_1},\ \mathrm{II}=\frac{1}{\eta_2}\left[\left(\frac{\partial\eta_2}{\partial t}\right)_{p_2}+\mathbf{v}_{H_2}\cdot(\nabla_H\eta_2)_{p_2}\right]=\frac{1}{\eta_2}\cdot A_2$$

and

$$\mathrm{III}=\frac{\eta_2}{\eta_1}\cdot\frac{1}{\eta_1}\left[\left(\frac{\partial\eta_1}{\partial t}\right)_{p_1}+\mathbf{v}_H\cdot(\nabla_{H_1}\eta_1)_{p_1}\right]=\frac{\eta_2}{\eta_1}\frac{1}{\eta_1}\cdot A_1.$$

An investigation will now be made into the values of these terms, partly with the true absolute vorticity, and partly with the geostrophic vorticity. The variation of f between two gridpoints will here be neglected. The following can be written: $\zeta=k\zeta_g$, $\eta=k\zeta_g+f$ and $\eta_g=\zeta_g+f$ and the expressions obtained for comparison purposes are as shown in Table 1.

We can, for example, further choose two groups of numerical values of k and ζ_g and calculate the error for every group. The result is shown in Table 2, where it can be seen that for so great a deviation as 30 % in the true wind from the geostrophic wind and for the values of f and $2f$ respectively of the geostrophic relative vorticities the relative errors in the terms I to III become 6, 12 and 23 % respectively. If the vorticity value increases, the relative error decreases rapidly. Depending on the varying sign and size of the different terms it can be said that the errors which result from these approximations probably do not exceed 10–15 % of the finally computed vertical velocity. To these errors should be added another error which can arise with varying values of k in the vertical, i.e. $k_1 \neq k_2$. When the error is then integrated upwards it could result in particularly uncertain values at 300 and 200 mb.

Another problem which has to be considered in this connection is the choice of a suitable grid distance for the computations of the geostrophic vorticity utilizing finite differences.

TABLE 2. *Examples of the relative errors in the terms in Table 1.*

Numerical values	Term	Geostrophical values	True values	Error in %
$k\approx0.7$	I	1.5	1.41	6
$\zeta_{g_1}\approx f$	II	$0.33\cdot A_2\cdot\frac{1}{f}$	$0.29\cdot A_2\cdot\frac{1}{f}$	12
$\zeta_{g_2}\approx 2f$	III	$0.75\cdot A_1\cdot\frac{1}{f}$	$0.58\cdot A_1\cdot\frac{1}{f}$	23
$k\approx0.7$	I	1.33	1.29	3
$\zeta_{g_1}\approx 2f$	II	$0.25\cdot A_2\cdot\frac{1}{f}$	$0.23\cdot A_2\cdot\frac{1}{f}$	8
$\zeta_{g_2}\approx 3f$	III	$0.44\cdot A_1\cdot\frac{1}{f}$	$0.37\cdot A_1\cdot\frac{1}{f}$	16

The vorticity field in the stream patterns contains different scales each of which must be described by a certain maximum grid distance. If this distance is exceeded the absolute vorticity becomes under-estimated and becomes more and more representative of phenomena on a larger scale. Through the suitable choise of grid distance in relation to the scale of the phenomenon that is being studied and to the size of the actual moving system on the map, the error which arises from the passage from differentials to differences may be decreased considerably.

In computing the geostrophic vorticity, in this case at the points A–D, a grid distance of 2 latitude degrees has been used.

In computing the advectional terms, $\mathbf{v}_H \cdot (\nabla_H \eta)_p$, in equation (3) the isobaric gradient of the absolute vorticity is determined from the field of geostrophic absolute vorticity as described above and, except for the frictional layer, the wind has been replaced by the geostrophic wind determined from the height fields of the different pressure surfaces. This seems to be the most serious approximation in the calculations. Existing ageostrophic windcomponents over the different points and in the region in general during the period of investigation are extremely difficult to estimate. Studying for example the 500 mb maps, however, it can be pointed out that a strong cyclonic curvature of the contour-lines (isohypses) in the region in question does not necessarily mean a strong ageostrophic departure of the true wind.

In order to describe the vorticity advection satisfactorily and to avoid too great smoothing the geostrophic wind has been computed with a grid distance of one latitude degree.

C. The vertical velocity reckoned as an average value during 6 hours

The absolute vorticity η, as well as its transport $\mathbf{v}_H \cdot (\nabla_H \eta)_p$, represent instantaneous values in the way they were calculated from the maps. Also, the local change of the absolute vorticity $(\partial\eta/\partial t)_p$ can naturally be determined approximately as an instantaneous value, and consequently even ω finally will result as an instantaneous value. However, in order to smooth the results to a certain extent, in this case ω has been calculated as an average value during a six-hour period (or as a representative value which applies to the time just in between two observations). Furthermore, average values are needed for computing, e.g. precipitation being based on the mean divergence during a certain time.

The term η_2, when inserted into equation (3), has been given the value $\frac{1}{2}[(\eta_2)_{t_0} + (\eta_2)_{t_0+6}]$, where t_0 is the time for the first observation, and $t_0 + 6$ is the time for observation 6 hours later. Similar expressions are used for the other terms. Thus the local changes can be replaced by $[(\eta)_{t_0+6} - (\eta)_{t_0}]/6$ hours. This way of procedure can however lead to a bad description of the change under certain circumstances, and for some control (η, t)-curves are constructed with the help of the vorticity analyses on the maps and in the cross-sections, and the local change is in the proper way thus derived from these curves.

D. The frictional effects upon the values of η and $\mathbf{v}_H \cdot (\nabla_H \eta)_p$ at the lower boundary, i.e. at the 1000 mb level

As previously mentioned the description of the computing method is valid for the free atmosphere and frictional effects have been neglected. Concerning the conditions at 1000 mb it is evident that the geostrophic approximation means too great an over-estimation both in the absolute vorticity and the advectional term. An over-estimation which affects the vertical velocity at all levels owing to the integration from below and upwards. With integration from 1000 mb to 850 mb the formula for calculating ω_{850} appears as follows if frictional effects are neglected:

$$\omega_{850} = -\eta_{g_{850}}(1000 - 850)\,\tfrac{1}{2}\left\{\frac{1}{\eta^2_{g_{850}}}\left[\left(\frac{\partial \eta_g}{\partial t}\right)_{850} + (\mathbf{v}_g \cdot \nabla_H \eta_g)_{850}\right] + \underbrace{\frac{1}{\eta^2_{g_{1000}}}\left[\left(\frac{\partial \eta_g}{\partial t}\right)_{1000} + (\mathbf{v}_g \cdot \nabla_H \eta_g)_{1000}\right]}_{C.}\right\}.$$

The last term C, in brackets, will now be reduced, bearing in mind the frictional effects, which imply partly a reduction of and partly a directional departure from the geostrophic winds computed from the 1000 mb height field.

TABLE 3. *A comparison between calculations using geostrophical values (g) and specially reduced values (r) respectively in representing the windfield in the 1000 mb level.*

Point A, 24th Sept. 0600–1200 GMT ($k \approx \frac{1}{3}$)				
Pressure surface	w cm sec^{-1} g	w cm sec^{-1} r	$(\mathrm{Div}_H\, \mathbf{v})_p$ 10^5 sec^{-1} g	$(\mathrm{Div}_H\, \mathbf{v})_p$ 10^5 sec^{-1} r
1000	0	0		
			−12.8	−7.3
850	+19	+11		
			−4.3	−4.7
700	+31	+21		
			−0.2	−0.3
500	+42	+30		
			+5.7	+5.7
300	+37	+18		

Point D, 24th Sept. 1200–1800 GMT ($k \approx \frac{2}{3}$)				
Pressure surface	w cm sec^{-1} g	w cm sec^{-1} r	$(\mathrm{Div}_H\, \mathbf{v})_p$ 10^5 sec^{-1} g	$(\mathrm{Div}_H\, \mathbf{v})_p$ 10^5 sec^{-1} r
1000	0	0		
			+5.9	+2.1
850	−9	−3		
			−2.6	−3.0
700	−6	+1.5		
			−0.5	−2.5
500	−6	+10		
			+4.7	+4.5
300	−33	−6.5		

This later deviation in the direction, if unitary in the whole considered region (determined by the grid distance chosen), does not change the value of the relative vorticity, as was earlier pointed out. In the advectional term the deviation in question, however, is to a certain extent of importance for the magnitude of the term. If it is also possible to take into account this deviation in wind direction when calculating the reduction of the term, in this case only the deviation in the absolute value of the wind is considered which without doubt is the most important source of error.

The reduction of C, depending on the deviation in magnitude of the wind from the geostrophic wind, is now carried out as follows. The assumption is made that $|\mathbf{v}| \approx k|\mathbf{v}_g|$ and the constant k is defined according to $k = |\mathbf{v}_{\text{obs}}|/|\mathbf{v}_g|$, where $\mathbf{v}_{\text{obs}}$ is an observed wind velocity representative of the area, and $\mathbf{v}_g$ is the geostrophic wind measured from the 1000 mb analyses. (The roughly approximated values recommended elsewhere of the reduction factor k in computing true wind values from the geostrophic wind at the anemometer level, i.e. $k \approx \frac{2}{3}$ over the sea and $k \approx \frac{1}{3}$ over the land, seem to be in good agreement with the values of k obtained according to the formula assumed.) From $|\mathbf{v}| \approx k|\mathbf{v}_g|$ we get $\zeta \approx k\zeta_g$ and further $(\partial\eta/\partial t)_p = (\partial\zeta/\partial t)_p \approx k\,(\partial\zeta_g/\partial t)_p$ and $\mathbf{v}_H \cdot (\nabla_H \eta)_p \approx k^2 \mathbf{v}_g \cdot (\nabla_H \zeta_g)_p$ where in the last term the variation of f with latitude in this case can be neglected. Now, in the term C, η_{g1000}, $(\partial\eta_g/\partial t)_{1000}$ and $(\mathbf{v}_g \cdot \nabla_H \eta_g)_{1000}$ can be replaced in this manner by their reduced expressions and so will appear as follows:

$$C \approx \frac{1}{(k\zeta_{g_{1000}} + f)^2}\left[k\left(\frac{\partial \zeta_g}{\partial t}\right)_{1000} + k^2(\mathbf{v}_g \cdot \nabla_H \zeta_g)_{1000}\right].$$

Naturally the reductional effects can now be discussed for different assumptions concerning the magnitudes of k and ζ_g in relation to f. The results of the reductions will however be illustrated as in Table 3 with the help of a couple of examples. The table shows the calculated results from the two points A and D (see Figs. 8 and 9) in which w (re-calculated from ω with the aid of formula (4)) and the isobaric divergence are calculated, both with the geostrophical computed values (with the notation g) and with the above described reductional procedure (with the notation r). From the results it can be seen that the vertical velocity itself becomes considerably reduced and at point D it even changes sign at 700 and 500 mb. With regard to the divergence in general the reductions only influence the layer 1000–850 mb, but on the other hand here the reduction is considerable.

E. AN ATTEMPT TO CALCULATE AS A CONTROL THE VERTICAL VELOCITY AT THE TOP OF THE FRICTIONAL LAYER UTILIZING OBSERVED WINDS AT ANEMOMETER LEVEL

A correct value of the calculated vertical velocity, at the 850 mb level, is of great importance when it is integrated all the way up and thus to a high degree determines the values of the vertical velocities at higher levels.

As a more effective control for the method described in section D, in taking into account the frictional effects on the computation of the first ω-value at 850 mb, an attempt has been made to calculate a value of the vertical velocity at the top of the frictional layer from the observed wind data at anemometer level.

In Fig. 13, the winds at anemometer level

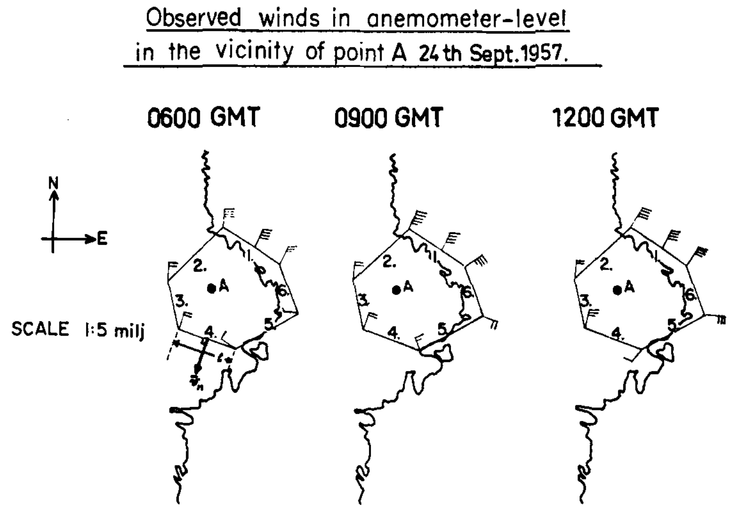

FIG. 13

in the vicinity of the point A are plotted for three observation times.

Proceeding from the equation of continuity, $(1/\varrho)\,(d\varrho/dt) = -\mathrm{Div}\ \mathbf{v}$, and neglecting the relative change in the density, which in this case would be small in proportion to the space derivatives of the wind, then $\partial w/\partial z = -\mathrm{Div}_H\mathbf{v}$. A rough calculation shows that the quantity $(1/\varrho)\,(d\varrho/dt)$ is one order of magnitude less than $(\partial w/\partial z)$ calculated according to the procedure in section D above. The following expression can now be written:

$$\int_0^z \frac{\partial w}{\partial z}\,\delta z = w_z = -\int_0^z \mathrm{Div}_H \mathbf{v}\cdot\delta z = -\int_0^z \frac{1}{A}\frac{dA}{dt}\,\delta z = -\int_0^z \left(\frac{1}{A}\oint_L v_n\,\delta l\right)\delta z.$$

Here, A is the horizontal cross sectional area of a vertical column of height z. δl is a line element on the circumference (L), and v_n is the wind component perpendicular to L and reckoned positive outwards from the area. The horizontally averaged value $\bar{w}_z$ of the vertical velocity at the height z over point A has been computed for the hexagon in Fig. 13 according to the following expression:

$$\bar{w}_z = -\frac{1}{A}\int_0^z\left(\sum_{i=1}^{6} \bar{v}_{n_i} l_i\right)\delta z = -\frac{1}{A}\sum_{i=1}^{6}\left(l_i\int_0^z \bar{v}_{n_i}\,\delta z\right) = -\frac{1}{A}\left(\sum_{i=1}^{6} l_i\,\tilde{\bar{v}}_{n_i}\right) z,$$

where $\sim$ indicates a vertically averaged value, $^{-}$ a horizontally averaged value along l and where the rough approximations $\tilde{\bar{v}}_n \approx \frac{1}{2}(\bar{v}_{n_0} + \bar{v}_{n_z})$ and $\bar{v}_{n_z} \approx a\ \bar{v}_{n_0}$ are made. The value of the a depends upon the change in magnitude as well as upon the change in direction of the wind inside the frictional layer. Further, $\bar{v}_{n_0}$ is calculated as an arithmetical mean value of the perpendicular wind component of the existing winds along every side of the hexagon.

First (at the time 0600 GMT), the wind vector is assumed constant with height, i.e. $a = 1$. Then, for $z = 1000$ m, the value $\bar{w}_{1000\ \mathrm{m}} = +11$ cm sec^{-1} and for $z = 1300$ m (≈ 850 mb) the value $\bar{w}_{850\ \mathrm{mb}} = +14$ cm sec^{-1} are obtained.

Thereafter it is assumed that the wind velocity varies linearly with height and a is set to 3/2 along the sides 1 and 6, by the Upplands coast, but for the rest a is set to 2. In this case the following values are obtained, $\bar{w}_{1000\ \mathrm{m}} = +10.5$ cm sec^{-1} and $\bar{w}_{850\ \mathrm{mb}} = +13$ cm sec^{-1}.

If a moderate change with height in the direction of the wind, unitary over the whole area, is taken into consideration a reduction is brought about of only less than 10 % of the computed values.

The computations for 0900 and 1200 GMT result in a less increase in the above given values, which perhaps qualitatively can be seen directly from Fig. 13.

In Fig. 8b it can be seen that the calculated value of the vertical velocity, according to the method given in section D, for point A at

850 mb is $\overline{w}_{850\text{ mb}} = +11$ cm sec^{-1}. Evidently the reductional procedure used does not seem to bring any error worth mentioning in the calculations of $w_{850\text{ mb}}$, not at least concerning the area surrounding point A.

4. The computed distributions of the vertical velocity and horizontal divergence at the points A, B, C and D, and a discussion of the results

The results of the computations have been illustrated in different forms in Figs. 8–11, where not only the distributions of the vertical velocity and horizontal divergence are made clear but also the positions of the points in question in relation to the frontal zone.

On the basis, among other things, of the soundings made at Gothenburg (Göteborg), Stockholm-Bromma, Helsinki (Helsingfors) and Tallin at 1200 GMT on 24th September, a vertical cross-section has been constructed shown in Fig. *8a*. The approximate position of the section is indicated in Fig. 7. Even if the intensity of the frontal zone cannot be exactly determined its existence is clearly verified by observations. The calculated vertical velocities at point C during the first six hours, 0600–1200 GMT have been used to represent the vertical velocities in the warm air in the vicinity of the frontal zone. The vertical motions of the cold air have been represented by the mean values for points A and B together during the same period (0600–1200 GMT). In addition to the fact that the precipitation distribution is in complete agreement with the computed vertical velocity distribution, which is further dealt with in the next section, the results are well supported by the observed humidity distribution. A low relative humidity, however, does not necessarily indicate a present downward directed motion. When the sounding at Bromma (Fig. 8) for example indicates a relative humidity in the frontal zone at 500 mb of about 10 % it can either be the result of a present vertical downward motion in the frontal zone or of an advection of dry air from the south which had then earlier been participating in a downward motion. In this case the calculated downward directed air motion at point C can explain the low relative humidity at Bromma.

Whereas the frontal zone over Stockholm during the period in question moved only very slowly eastwards, which has been commented upon earlier, the velocity of the frontal zone at point D was considerably greater. This can also be seen through studying Fig. 7 where the positions of the low pressure centre at 0600, 1200 and 1800 GMT is indicated both at 500 and 700 mb. In this figure the horizontal projections of the vertical cross-sections, which are constructed in Figs. *8a* and *9a*, are also illustrated. The calculated values of the vertical velocity at point D are uncertain since this point at time 1200 GMT on the whole lay in the frontal zone; the neglection of the "tilting-term" here would seem to be unjustified (see the derivation of equation (2) above). At the times 0600 and 1800 GMT, however, point D probably would have been entirely within the warm and cold air respectively. Since it is the mean values for the periods 0600–1200 and 1200–1800 GMT that have been found, it is then possible that the quality of the computations have not been too greatly affected. In Fig. *9a* the vertical velocity in the warm air has been represented by the values at point D during the period 0600–1200 GMT, and in the cold air north of the front, by the values at the same point during the period 1200–1800 GMT. The illustrated humidity values are based on the mean conditions at the front, calculated from the records of humidity with the passage of the frontal zone over Gothenburg (Göteborg), Copenhagen (Köpenhamn) and Schleswig (see Fig. 3). In this front section too, a relatively high value of the upward directed vertical velocity in the cold air has been obtained at 500 mb. In the lowest layer, however, downward air motions occur, which together with the humidity distribution, explain the complete absence of precipitation in this area (see Fig. 6).

The computations and direct observations at a certain front section thus clearly show a vertical circulation with ascending cold air and descending warm air. This kind of motion represents an energy consuming thermal indirect circulation. With only a cursory study of the currents' distributions (see for example Fig. 7) it seems that a great part of the energy source would be found in the horizontal kinetic energy on the greater scale of motion. A decrease in velocity of the air in the middle and upper regions of the troposphere is clearly noticeable when the air passes through the area south and east of the low pressure centre.

Perhaps as a matter of some interest it can finally be noticed that the level of non-divergence only appears at about 600 mb over the points A and B.

5. A calculation of the amounts of precipitation at points A and B using and thus controlling the distribution of the computed horizontal divergence

The precipitation, which falls in the areas surrounding points A and B (see Fig. 6) during the time 0600–1800 GMT on 24th September, has been computed using certain simplified assumptions. According to the observations the rain began before 0600 and continued until after 1800 GMT. The trajectories of the air particles inside the precipitation area were to a great extent directed from north to south in the lowest 3–5 km (see Fig. 7) and under these circumstances the relative humidity can be considered to be constant and at 100 % in the inner parts of the precipitation area, where points A and B are to be found. Furthermore, the temperature in the cold air in these areas can, to a certain degree, be regarded as approximately constant during the period in question. The maximum specific humidity has been calculated at different levels and inserted on the 0-lines in Figs. 8*b* and 10.

Considering an air column with constant maximum specific humidity for which the reasons are stated above the amount of condensed water vapor inside this column can be calculated directly from the horizontal divergence of the wind. Furthermore, it can be assumed that everything that is condensed falls out as precipitation in the inner parts of such a great area of rain, when such a long time interval with continuous precipitation is considered (see section 1 concerning the precipitation analysis).

Under the above discussed conditions the amount of precipitation P as a very good approximation can be calculated as follows, where $\bar{q} = \bar{q}_{\max}$ and $\bar{\varrho}$ are horizontally averaged values, in the small region in question, of the specific humidity and the density of the air respectively:

$$P \approx -\int_0^\infty \mathrm{Div}_H(\bar{q}_{\max}\bar{\varrho}\mathbf{v}) \cdot \delta z$$

$$= -\int_0^\infty \bar{q}_{\max}\bar{\varrho}\, \mathrm{Div}_H \mathbf{v} \cdot \delta z$$

$$= 220 \int_{p_0}^0 \bar{q}_{\max}\, \mathrm{Div}_H \mathbf{v} \cdot \delta p \text{ in } \frac{\text{mm}}{6\text{ hours}}$$

if q in g/kg, the divergence in sec^{-1} and p in mb. The integration can easily be carried out graphically or layer by layer from the divergence curve and numbers of specific humidity indicated in Figs. 8*b* and 10 up to about the 600–500 mb level, above which the contributions can be neglected. The precipitation has been calculated separately for every 6-hour period.

The precipitation at point A is found to be $P_{06-12} = 18.5$ mm and $P_{12-18} = 14$ mm or a total of 33 mm. For point B the corresponding values are 9.5 and 3.5, or a total of 13 mm.

The order of size of the area which the computed values can be said to represent is probably the area of a circle having a radius of a little more than 50 km. It is, however, difficult to decide the exact size of that area since actually during all calculations different space and time averaged values are used.

According to Fig. 6, it is seen that in the areas around A and B the observed amounts of precipitation are almost exactly of the same magnitude as the calculated amounts. A rough estimation gives for A 30–35 mm and for B about 15 mm. Thus the observed results are in very good agreement with those from computations and this can be considered as a proof of the validity of the computed vertical velocities as well as of the computational procedure used at least in the rainy areas, i.e. the cold air.

Some concluding remarks

It was assumed, from the start of the investigation, that the denser networks, both in space and time, which were established during I.G.Y.'s meteorological world intervals, would have made it possible to describe with a desirable accuracy certain features of the three-dimensional structure of the atmosphere; for instance, a description of the dynamics and thermodynamics connected with such a cold and almost thermally symmetric cyclonic vortex which, actually during one of those world intervals, passed over Scandinavia, the track of which is indicated in Fig. 5. Several trials using different methods were also made in order to thus utilize the data material but most of them were abandoned and the investigation was finally restricted to the problem presented in this paper. The reason for this restriction lies in the strongly selective character of the different

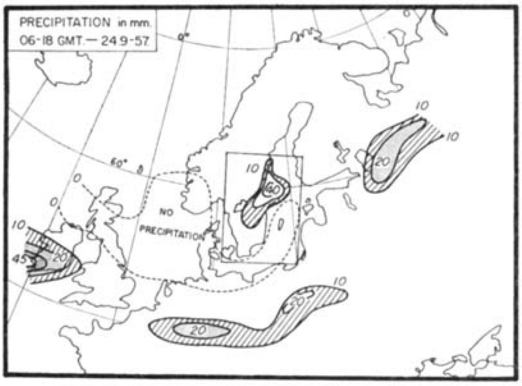

a

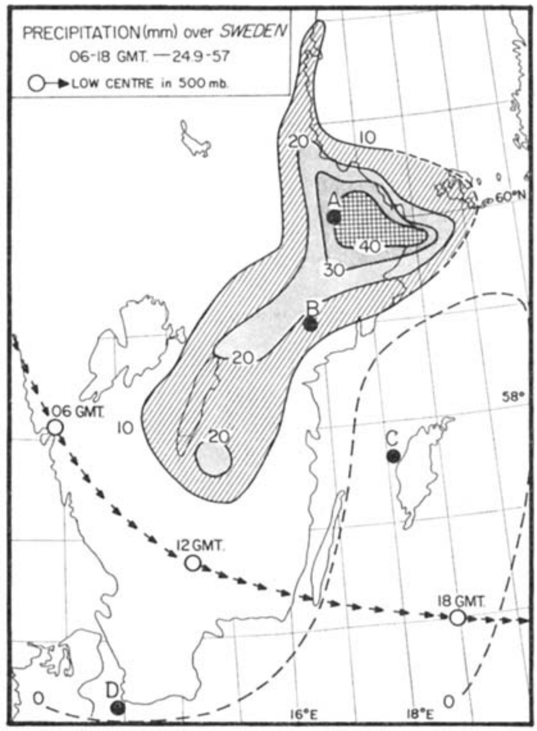

FIG. 6 *b*

THE POSITIONS OF THE POINTS A, B, C AND D IN RELATION TO THE FRONTAL ZONE, 24th SEPT. 1957.

THE NORTHERN FRONTAL ZONE AND THE POSITIONS OF THE LOW-CENTRE EVERY SIX HOURS ARE INDICATED.

—·—·— The positions of the cross-sections shown in the figures 8 and 9.

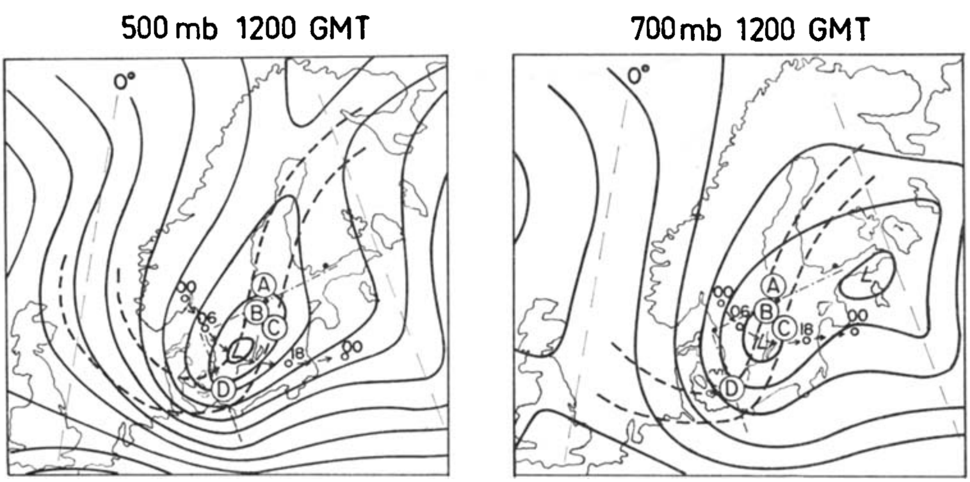

FIG. 7

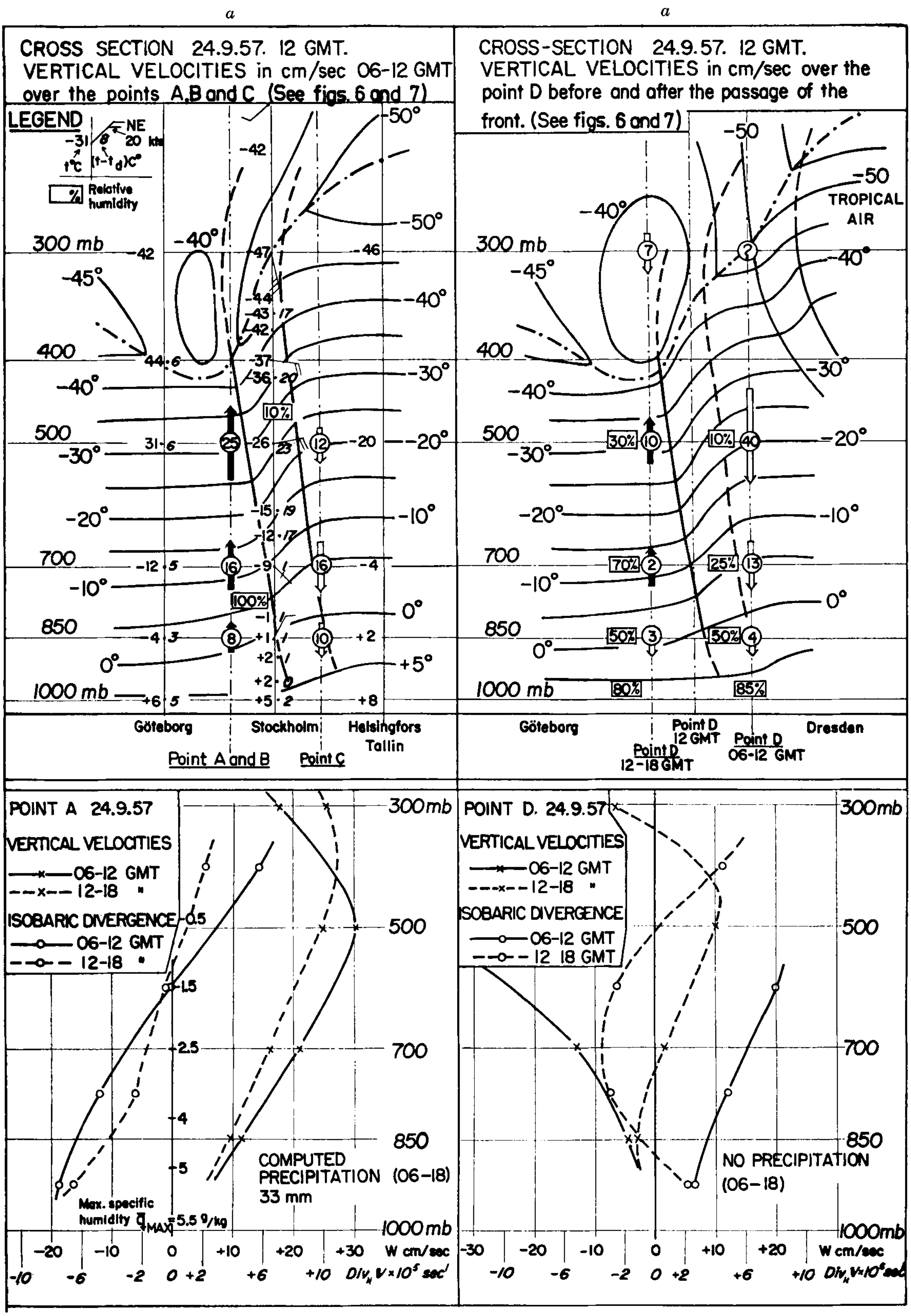

a
a
CROSS SECTION 24.9.57. 12 GMT.
VERTICAL VELOCITIES in cm/sec 06-12 GMT over the points A,B and C (See figs. 6 and 7)
LEGEND
Relative humidity
300 mb
400
500
700
850
1000 mb
Göteborg
Stockholm
Helsingfors Tallin
Point A and B
Point C
CROSS-SECTION 24.9.57. 12 GMT.
VERTICAL VELOCITIES in cm/sec over the point D before and after the passage of the front. (See figs. 6 and 7)
TROPICAL AIR
Point D 12 GMT
Point D 12-18 GMT
Point D 06-12 GMT
Dresden
POINT A 24.9.57
VERTICAL VELOCITIES
06-12 GMT
12-18 "
ISOBARIC DIVERGENCE
06-12 GMT
12-18 "
COMPUTED PRECIPITATION (06-18) 33 mm
Max. specific humidity q_{MAX}=5.5 g/kg
W cm/sec
$Div_H V \times 10^5 sec^{-1}$
POINT D. 24.9.57
VERTICAL VELOCITIES
06-12 GMT
12-18 "
ISOBARIC DIVERGENCE
06-12 GMT
12 18 GMT
NO PRECIPITATION (06-18)
b
b

FIG. 8

FIG. 9

Fig. 10

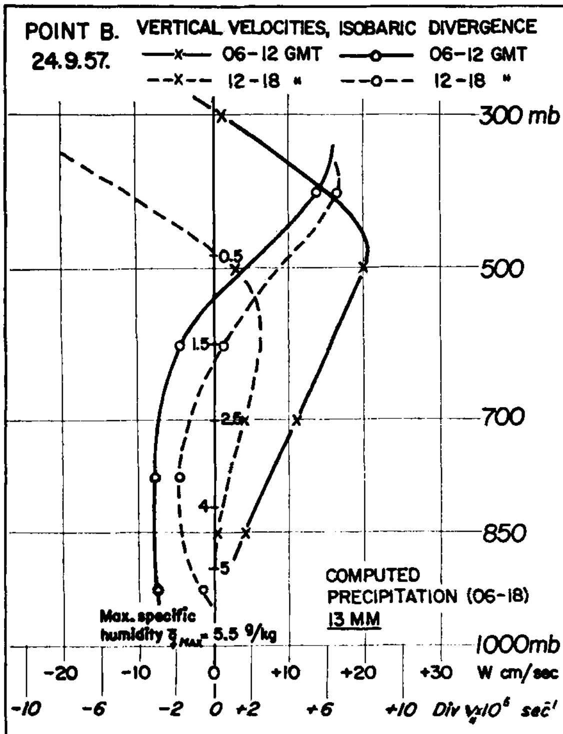

Fig. 11

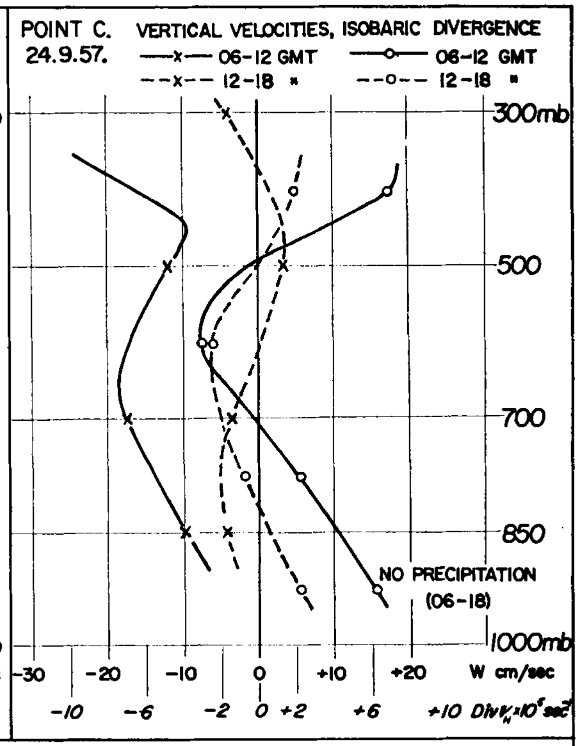

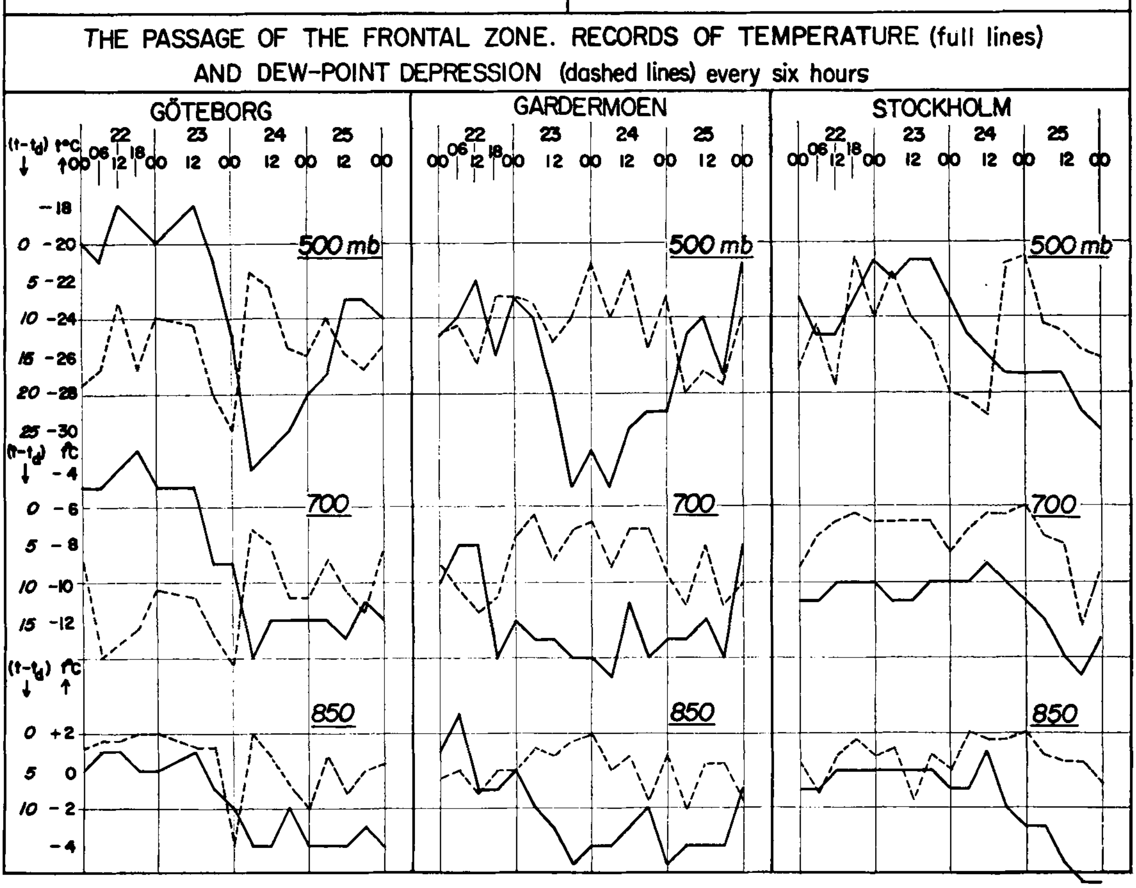

Fig. 12

available computing methods concerning the vertical velocity and thereby also in the heavy demands which must be made on the observational material. If, in addition, the calculated values are required to be clearly verified, then the number of points where computations can be used will be further considerably reduced. Moreover, the time-scale of the variations of the sought-after property has to be at least of the same order of magnitude as the observational time interval. The processes also naturally have to take place just in those regions having a sufficiently dense space network. Finally, if furthermore it is desired to state a closer relation between a certain process and a certain phenomenon in time and space, for instance a vertical circulation in relation to a frontal zone, the space-scale of which is small compared with the distance between the aerological stations, the possibilities of successful results are further strongly reduced.

The present investigation shows in many ways the several difficult problems which meet the meteorologist in investigating the atmosphere and especially in the case of passing from the large-scale features to the detailed structure on the smaller synoptical scale. The discovered vertical circulations, having all precipitation generated in the upward moving cold air and with dry air on the warmer side of a special front-section, may certainly not be generalized, but it is perhaps a more usual type of circulation at certain sections of the tropospherical fronts than was previously believed.

Acknowledgements

The basic work of the investigation presented above was carried out during the author's participation in a smaller Scandinavian working-group, which was established in Oslo during the I.G.Y. The author now takes the opportunity of thanking Director R. Fjörtoft and Norsk Meteorologisk Institutt for placing a number of assistants at the group's disposal. He also wishes to thank those staff members who prepared the data material, and his collaborator, the senior state meteorologist P. M. Breistein, for valuable advice and discussions. Furthermore the author is indebted to Professors B. Bolin and E. Palmén for their active interest and helpful criticisms made during the investigation.